

Detailed analysis of the chiral unitary model for meson-baryon scatterings with flavor SU(3) breaking effects

Tetsuo HYODO¹, Seung-il NAM^{1,2}, Daisuke JIDO^{1*)} and Atsushi HOSAKA¹

¹*Research Center for Nuclear Physics (RCNP), Ibaraki, Osaka 567-0047, Japan*

²*Department of Physics, Pusan National University, Pusan 609-735, Korea*

We study s -wave meson-baryon scatterings using the chiral unitary model. We consider $1/2^-$ baryon resonances as quasibound states of the low lying mesons (π, K, η) and baryons (N, Λ, Σ, Ξ). In previous works, the subtraction constants which appeared in loop integrals largely depended on channels and it was necessary to fit these constants to reproduce the data. In order to extend this model to all channels with fewer parameters, we introduce flavor SU(3) breaking interactions in the framework of chiral perturbation theory. It is found, however, that the observed SU(3) breaking in meson-baryon scatterings cannot be explained by the present SU(3) breaking interactions. The role and importance of the subtraction constants in the present framework are discussed.

§1. Introduction

The study of meson-baryon scatterings of various channels in a unified way is important to understand hadron dynamics at low and intermediate energy regions from the viewpoint of QCD. Especially the properties of excited states of baryons observed in the meson-baryon scatterings as resonances are investigated with great interest both theoretically and experimentally. So far, there are several established approaches to describe the properties of the baryon resonances. A recent development in this field is the introduction of the chiral unitary model,^{1),2),3),4),5),6)} where the s -wave baryon resonances are dynamically generated in meson-baryon scatterings, while the conventional quark model approach describes the baryon resonances as three-quark states with an excitation of one of the quarks.

The chiral unitary model is based on the chiral perturbation theory (ChPT).^{7),8)} Imposing the unitarity condition, we can apply the ChPT at higher energy region than in the original perturbative calculation, and we can study properties of resonances generated by non-perturbative resummations. In the implementation of the unitarity condition, regularization of loop integrals brings parameters into this model, such as the three-momentum cut-off and the “subtraction constants” in the dimensional regularization.

In Refs. 1),5), the s -wave scatterings of the meson and baryon systems with the strangeness $S = -1$ were investigated by solving the Lippman-Schwinger equation in the coupled channels, where the $\Lambda(1405)$ resonance was dynamically generated by the meson-baryon scatterings. In the regularization procedure, parameters were introduced for the finite ranges in the kernel potential,¹⁾ and for the three-momentum cut-off in the loop integral.⁵⁾ In Refs. 9), 10), 11), they extended the chiral uni-

^{*)} Present address: ECT*, European Centre for Theoretical Studies in Nuclear Physics and Related Areas Villa Tambosi, Strada delle Tabarelle 286, I-38050 Villazzano (Trento), Italy

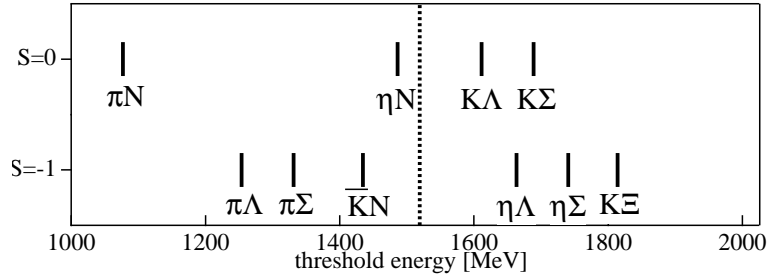


Fig. 1. Threshold energies of the meson-baryon scatterings in the $S = -1$ and $S = 0$ channels.
The dotted line in the middle represents the averaged energy of all meson-baryon thresholds.

tary approach to other strangeness channels and obtained the baryonic resonances, $\Lambda(1405)$, $N(1535)$, $\Lambda(1670)$, $\Sigma(1620)$ and $\Xi(1620)$, as dynamically generated objects. They used the dimensional regularization scheme with channel dependent subtraction constants (a_i 's). In particular, the subtraction constants in $S = 0$ depended significantly on channels, while as reported in Ref. 12), a common subtraction constant was found in the $S = -1$ channel to reproduce the total cross sections of the K^-p scattering as well as $\Lambda(1405)$ properties. Note also that in a similar model with different regularization scheme,¹³⁾ the position of the poles and their properties are changed.

In this work, we raise a question whether such channel dependence of subtraction constants could be dictated by the flavor SU(3) breaking effects of an underlying theory, or not. As we will discuss in detail, it is shown that the subtraction constants should not be dependent on scattering channels in the SU(3) limit.^{14),15)} The SU(3) breaking should have significant effects on observed quantities. This is expected from, for instance, the large dependence of the threshold energies on the meson-baryon channels as shown in Fig. 1. This is particularly the case for $S = 0$, where the lowest threshold energy of the πN channel deviates considerably from the mean value. Furthermore, it was discussed in Ref. 16) that the number of the channel dependent subtraction constants for all SU(3) channels exceeds the number of available counter terms of chiral order p^3 .

In order to study the above questions, we consider the following two cases;

- We use a common subtraction constant for all scattering channels and see whether this simplified calculation works or not.
- When this method does not work, we introduce the flavor SU(3) breaking effects in the interaction kernel.

In this way, we expect that the free parameters in the previous works could be controlled with suitable physics ground, which allows us to extend this method to other channels with predictive power. Note that the use of single subtraction constant was first examined in Ref. 17). In this work, we concentrate on the s wave scatterings, since the p wave contribution to the total cross sections is shown to be small in the $S = -1$ channel in Ref. 18).

This paper is a detailed study of the results in Ref. 15). In section 2, we present the formulation of the chiral unitary model. The calculation with a common sub-

traction constant and comparison with the previous works are shown in section 3. We then introduce the flavor SU(3) breaking effects in the interaction kernel and present numerical results in section 4. We discuss the results and summarize this work in section 5.

§2. Formulation

In this section we review briefly the formulation of the chiral unitary model. We derive the basic interaction of meson-baryon scatterings from the lowest order chiral Lagrangian, and we maintain the unitarity of the S-matrix. There are several methods which recover the unitarity of the S-matrix such as solving the Bethe-Salpeter Equation (BSE),⁵⁾ Inverse Amplitude Method (IAM),¹⁹⁾ N/D method¹²⁾ and so on. In this work, we adopt the N/D method,²⁰⁾ since this method provides a general form of the T-matrix using the dispersion relation and the analyticity of inverse of the T-matrix. Recently the N/D method has been applied to coupled channel meson-baryon scatterings.^{21),12)} It was found that the final form of the T-matrix derived from the N/D method is essentially equivalent to the result of Ref. 5) derived from the BSE.

The chiral Lagrangian for baryons in the lowest order of the chiral expansion is given by²²⁾

$$\mathcal{L}_{\text{lowest}} = \text{Tr} \left(\bar{B} (i \not{D} - M_0) B - D (\bar{B} \gamma^\mu \gamma_5 \{A_\mu, B\}) - F (\bar{B} \gamma^\mu \gamma_5 [A_\mu, B]) \right). \quad (2.1)$$

Here D and F are coupling constants. In Eq. (2.1) the covariant derivative \mathcal{D}_μ , the vector current V_μ , the axial vector current A_μ and the chiral field ξ are defined by

$$\mathcal{D}_\mu B = \partial_\mu B + i[V_\mu, B], \quad (2.2)$$

$$V_\mu = -\frac{i}{2} (\xi^\dagger \partial_\mu \xi + \xi \partial_\mu \xi^\dagger), \quad (2.3)$$

$$A_\mu = -\frac{i}{2} (\xi^\dagger \partial_\mu \xi - \xi \partial_\mu \xi^\dagger), \quad (2.4)$$

$$\xi(\Phi) = \exp\{i\Phi/\sqrt{2}f\}, \quad (2.5)$$

where f is the meson decay constant, here we take an averaged value $f = 1.15f_\pi$ with $f_\pi = 93$ MeV. The meson and baryon fields are expressed in the SU(3) matrix form as

$$B = \begin{pmatrix} \frac{1}{\sqrt{2}}\Sigma^0 + \frac{1}{\sqrt{6}}\Lambda & \Sigma^+ & p \\ \Sigma^- & -\frac{1}{\sqrt{2}}\Sigma^0 + \frac{1}{\sqrt{6}}\Lambda & n \\ \Xi^- & \Xi^0 & -\frac{2}{\sqrt{6}}\Lambda \end{pmatrix}, \quad (2.6)$$

$$\Phi = \begin{pmatrix} \frac{1}{\sqrt{2}}\pi^0 + \frac{1}{\sqrt{6}}\eta & \pi^+ & K^+ \\ \pi^- & -\frac{1}{\sqrt{2}}\pi^0 + \frac{1}{\sqrt{6}}\eta & K^0 \\ K^- & \bar{K}^0 & -\frac{2}{\sqrt{6}}\eta \end{pmatrix}. \quad (2.7)$$

In the Lagrangian (2.1), M_0 denotes a common mass of the octet baryons. However, we use the observed values of the baryon masses in the following calculations. The

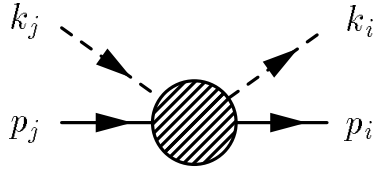


Fig. 2. Definition of the momentum variables. Dashed and solid lines represent mesons and baryons, respectively.

mass splitting among the octet baryons in the Lagrangian level will be introduced consistently with the SU(3) breaking in section 4.

The s wave interactions at the tree level come from the Weinberg-Tomozawa (WT) interaction, which is in the vector coupling term in the covariant derivative;

$$\mathcal{L}_{WT} = \text{Tr} \left(\bar{B} i \gamma^\mu \frac{1}{4f^2} [(\Phi \partial_\mu \Phi - \partial_\mu \Phi \Phi), B] \right). \quad (2.8)$$

From this Lagrangian, the meson-baryon scattering amplitude at the tree level is given by

$$\begin{aligned} V_{ij}^{(WT)} &= -\frac{C_{ij}}{4f^2} \bar{u}(p_i)(\not{k}_i + \not{k}_j)u(p_j) \\ &= -\frac{C_{ij}}{4f^2} (2\sqrt{s} - M_i - M_j) \sqrt{\frac{E_i + M_i}{2M_i}} \sqrt{\frac{E_j + M_j}{2M_j}}, \end{aligned} \quad (2.9)$$

where the indices (i, j) denote the channels of the meson-baryon scatterings and M_i and E_i are the mass and the energy of the baryon in the channel i , respectively. These masses and factors come from the spinors of the baryons. It seems to be reasonable to use the common mass M_0 in the Lagrangian as in Ref. 12), however, in this paper we adopt the physical masses as in Refs. 9), 10), 11). Indeed we have checked that the results with a common mass are qualitatively similar to the results with observed masses. The channels (i, j) are shown in Table III in Appendix. The kinematics of this vertex is shown in Fig. 2 and s in Eq. (2.9) is defined as $s = (k + p)^2$. The last line is obtained in the center of mass frame with the nonrelativistic reduction. The coefficient C_{ij} is fixed by chiral symmetry and the explicit form of C_{ij} is shown in Ref. 5) for $S = -1$ and in Ref. 10) for $S = 0$.

In the coupled channel formulation the T-matrix takes a matrix form. The unitarity condition is guaranteed by the optical theorem $-2\text{Im}[T_{ii}] = T_{ik}\rho_k T_{ki}^*$, which can be written as

$$2\text{Im}[T_{ii}^{-1}] = \rho_i, \quad (2.10)$$

where the normalization of the T-matrix is defined by

$$S_{ij} = 1 - i \left(\frac{\sqrt{2M_i}|\mathbf{q}_i|2M_j|\mathbf{q}_j|}{4\pi\sqrt{s}} \right) T_{ij}$$



Fig. 3. Diagrammatic interpretation of Eq. (2.18).

With the condition (2.10) and the dispersion relation for T_{ii}^{-1} , we find a general form of the T-matrix using the N/D method. Following Ref. 12), we write

$$T_{ij}^{-1}(\sqrt{s}) = \delta_{ij} \left(\tilde{a}_i(s_0) + \frac{s - s_0}{2\pi} \int_{s_i^+}^{\infty} ds' \frac{\rho_i(s')}{(s' - s)(s' - s_0)} \right) + \mathcal{T}_{ij}^{-1}, \quad (2.11)$$

where s_i^+ is the value of s at the threshold of the channel i , and s_0 is the subtraction point. The parameter $\tilde{a}_i(s_0)$ is the subtraction constant and is a free parameter within the N/D method. The matrix \mathcal{T}_{ij} is determined by the chiral perturbation theory as discussed later. In the derivation of Eq. (2.11), we have neglected the left hand cuts, which correspond to u -channel diagrams of the crossing symmetry.

Let us assume that the intermediate states of the meson-baryon scatterings are composed by one octet meson and one octet baryon. We do not consider multi-mesons and excited baryons, such as $\pi\pi N$ and $\pi\Delta$. In this case, the phase space ρ_i in Eq. (2.10) is written as

$$\rho_i(\sqrt{s}) = \frac{2M_i|\mathbf{q}_i|}{4\pi\sqrt{s}}, \quad (2.12)$$

where \mathbf{q}_i is a three-momentum of the intermediate meson on the mass shell. Let us define the G function by

$$G_i(\sqrt{s}) = -\tilde{a}_i(s_0) - \frac{s - s_0}{2\pi} \int_{s_i^+}^{\infty} ds' \frac{\rho_i(s')}{(s' - s)(s' - s_0)}, \quad (2.13)$$

which takes the same form as, up to a constant, the ordinary meson-baryon loop function:

$$G_i(\sqrt{s}) = i \int \frac{d^4 q}{(2\pi)^4} \frac{2M_i}{(P - q)^2 - M_i^2 + i\epsilon} \frac{1}{q^2 - m_i^2 + i\epsilon}. \quad (2.14)$$

This integral should be regularized by an appropriate regularization scheme. In the dimensional regularization, the integral is calculated as

$$\begin{aligned} G_i(\sqrt{s}) = & \frac{2M_i}{(4\pi)^2} \left\{ a_i(\mu) + \ln \frac{M_i^2}{\mu^2} + \frac{m_i^2 - M_i^2 + s}{2s} \ln \frac{m_i^2}{M_i^2} \right. \\ & + \frac{\bar{q}_i}{\sqrt{s}} \left[\ln(s - (M_i^2 - m_i^2) + 2\sqrt{s}\bar{q}_i) + \ln(s + (M_i^2 - m_i^2) + 2\sqrt{s}\bar{q}_i) \right. \\ & \left. \left. - \ln(-s + (M_i^2 - m_i^2) + 2\sqrt{s}\bar{q}_i) - \ln(-s - (M_i^2 - m_i^2) + 2\sqrt{s}\bar{q}_i) \right] \right\}, \end{aligned} \quad (2.15)$$

channel dependent a_i ($S = -1$)						
channel	$\bar{K}N$	$\pi\Sigma$	$\pi\Lambda$	$\eta\Lambda$	$\eta\Sigma$	$K\Xi$
a_i	-1.84	-2.00	-1.83	-2.25	-2.38	-2.67

channel dependent a_i ($S = 0$)				
channel	πN	ηN	$K\Lambda$	$K\Sigma$
a_i	0.711	-1.09	0.311	-4.09

Table I. Channel dependent subtraction constants a_i used in Refs. 9), 10) with the regularization scale $\mu = 630$ MeV. For the $S = 0$ channel, although the original values of a_i are obtained with $\mu = 1200$ MeV, here we show the values of a_i corresponding to $\mu = 630$ MeV by using the relation $a(\mu') = a(\mu) + 2\ln(\mu'/\mu)$.

where μ is the regularization scale, a_i is the subtraction constant and \bar{q}_i is defined by

$$\bar{q}_i(\sqrt{s}) = \frac{\sqrt{(s - (M_i - m_i)^2)(s - (M_i + m_i)^2)}}{2\sqrt{s}}. \quad (2.16)$$

In the tree approximation, only the \mathcal{T}_{ij} term survives in Eq. (2.11), which may be identified with the WT interaction $V^{(WT)}$ in Eq. (2.9). Therefore, the resulting T-matrix is written as

$$T^{-1} = -G + (V^{(WT)})^{-1}, \quad (2.17)$$

$$T = V^{(WT)} + V^{(WT)}GT. \quad (2.18)$$

This is the algebraic equation for the T-matrix, which corresponds to the integral BSE. The diagrammatic interpretation of Eq. (2.18) is shown in Fig. 3.

The subtraction constants $a_i(\mu)$ in Eq. (2.15), in principle, would be related to the counter terms in the higher order Lagrangian in the chiral perturbation theory. In the previous works,^{9), 10)} they have fitted these subtraction constants(a_i) by using the data of $\bar{K}N(S = -1)$ and $\pi N(S = 0)$ scatterings. In Table I we show the subtraction constants used in Refs. 9), 10). In the table, in order to compare the channel dependence of the subtraction constants, we take the regularization scale at $\mu = 630$ MeV in the both channels. Changing the regularization scale, the subtraction constants are simply shifted by $a(\mu') = a(\mu) + 2\ln(\mu'/\mu)$. From this table we see that the a_i values in $S = 0$ are very much different from each other. In the rest of this paper we refer to these parameters as “channel dependent a_i ”.

§3. Calculation with a common subtraction constant

In this section, we show calculations in which a single subtraction constant a is commonly used in the meson-baryon loop function (2.15), in order to see the role of the channel dependent a_i to reproduce the observed cross sections and the resonance properties. Channel independent regularization scheme was first used in Ref. 17).

Let us first show that in the SU(3) limit together with the constraint in the chiral unitary model, there is only one subtraction constant.^{14), 15)} Under SU(3) symmetry, scattering amplitudes of one octet meson and one octet baryon are composed of SU(3)

irreducible representations. The amplitudes satisfy the scattering equation in each representation,

$$T(D) = V(D) + V(D)G(D)T(D) , \quad (3.1)$$

where D represents an SU(3) irreducible representation, $D = 1, 8, 8, 10, \bar{10}$ and 27. Therefore, on one hand, the functions G , or equivalently the subtraction constants a_i are represented by diagonal matrices in the SU(3) basis. On the other hand, since G functions are given as a loop integrals as shown in (14) and (15), they are also diagonal in the particle basis $(\pi^- p, \eta A, \dots)$. These observations imply that the subtraction constants are components of a diagonal matrix both in SU(3) and particle bases, which are transformed uniquely by a unitary matrix of SU(3) Clebsch-Gordan coefficients;

$$a(D) = \sum_k U_{Dk} a_k (U^\dagger)_{kD} . \quad (3.2)$$

This can be happen when the subtraction constants is proportional to unity. Hence, subtraction constants are not dependent on channels in the SU(3) limit.

Now, we discuss the case of $S = -1$, where the subtraction constants a_i are not very dependent on the channels as shown in Table I. Therefore, it is expected that the calculation with a common a gives a good description by choosing a suitable value.

Next we study the $S = 0$ channel using a common subtraction constant. Here we will find that the common a cannot reproduce simultaneously the resonance properties and the S_{11} amplitude at low energy region.

In order to concentrate on the role of the subtraction constants and to see the channel dependence, we assume the following simplifications for the calculations of the $S = -1$ and $S = 0$ channels;

- We use an averaged value for the meson decay constants, $f = 1.15f_\pi = 106.95$ MeV, while in Ref. 10) physical values were taken as $f_\pi = 93$ MeV, $f_K = 1.22f_\pi$, $f_\eta = 1.3f_\pi$.
- We do not include the effect of vector meson exchanges and $\pi\pi N$ channels to reproduce the $\Delta(1620)$ resonance, which were considered in Ref. 10).

With these simplifications, the calculations in the $S = -1$ and $S = 0$ channels are based on exactly the same formulation; the differences are in the flavor SU(3) coefficients C_{ij} in Eq. (2.9) and in the channel dependent subtraction constants.

3.1. The $S = -1$ channel ($\bar{K}N$ scattering)

In the $S = -1$ channel, the subtraction constants a_i obtained in Ref. 9) are not very much dependent on the channels, as shown in Table I. In Ref. 12), they used a common $a \sim -2$, which was “naturally” obtained from the matching with the three-momentum cut-off regularization with $\Lambda = 630$ MeV. In the both works, they reproduced very well the total cross sections of the $K^- p$ scatterings and the mass distribution of the $\pi\Sigma$ channel with $I = 0$, where the $\Lambda(1405)$ resonance is seen. In Ref. 9), the $\Lambda(1670)$ resonance was also obtained with the channel dependent subtraction constants, and its property was discussed by analyzing the speed plots in the $I = 0$ channels.

Here we search one common a to be used in all channels in $S = -1$. In order to fix the common a , we use threshold properties of the $\bar{K}N$ scatterings, which are well observed in the branching ratios:^{23),24)}

$$\begin{aligned}\gamma &= \frac{\Gamma(K^- p \rightarrow \pi^+ \Sigma^-)}{\Gamma(K^- p \rightarrow \pi^- \Sigma^+)} \sim 2.36 \pm 0.04, \\ R_c &= \frac{\Gamma(K^- p \rightarrow \text{charged particles})}{\Gamma(K^- p \rightarrow \text{all})} \sim 0.664 \pm 0.011, \\ R_n &= \frac{\Gamma(K^- p \rightarrow \pi^0 \Lambda)}{\Gamma(K^- p \rightarrow \text{neutral particles})} \sim 0.189 \pm 0.015.\end{aligned}\quad (3.3)$$

After fitting, we find the optimal value $a = -1.96$, with which the threshold branching ratios are obtained as shown in Table II. The result using the common $a = -1.96$ does not differ very much from that of channel dependent ones, and also the value $a = -1.96$ is close to an averaged value of the channel dependent subtraction constants a_i , namely ~ -2.15 . Therefore, the threshold properties are not sensitive to such a fine tuning of the subtraction constants.

Using the common $a = -1.96$, we calculate the total cross sections of the $K^- p$ scatterings (Fig. 4, solid lines), the T-matrix amplitude of the $\bar{K}N$ scattering with $I = 0$ (Fig. 5, solid lines) and the mass distributions of the $\pi\Sigma$ channel with $I = 0$ (Fig. 6, solid lines). We also plot the calculations with the channel dependent a_i obtained in Ref. 9) in Figs. 4,5 and 6 as the dotted lines. Here we find that the present calculations are slightly different from the calculations with the channel dependent a_i in the total cross sections and the $\pi\Sigma$ mass distributions. Therefore, the $\Lambda(1405)$ resonance is well reproduced with the common $a = -1.96$, which is consistent with the results in Ref. 12). However, the resonance $\Lambda(1670)$ disappears when the common a is used, as we see in the T-matrix amplitude of $\bar{K}N \rightarrow \bar{K}N$ with $I = 0$ in Fig. 5. As pointed out in Ref. 9), the $\Lambda(1670)$ resonance structure is very sensitive to the value of $a_{K\Sigma}$. Indeed we have checked that the $\Lambda(1670)$ resonance is reproduced when we choose $a_{K\Sigma} \sim -2.6$ with the other a_i unchanged, -1.96 . In the recent publication, it was shown that the poles of $\Lambda(1405)$ and $\Lambda(1670)$ simultaneously were reproduced by taking into account the approximate crossing symmetry without considering explicitly the channel dependence 13). The inclusion of the crossing symmetry is, however, beyond our scope in the present discussion.

If we choose $a = -2.6$ for all subtraction constants, the threshold branching ratios are calculated as $\gamma = 2.41$, $R_c = 0.596$ and $R_n = 0.759$, and the agreement with the experimental data becomes poor, as shown in Figs. 4 and 5. In particular, the $K^- p \rightarrow \bar{K}^0 n$ cross section is underestimated, and also the resonance structure of $\Lambda(1405)$ disappears in the $\pi\Sigma$ mass distribution (Fig. 6). As we change all subtraction constants from $a = -1.96$ to $a = -2.6$ gradually, the position of the peak of $\Lambda(1405)$ moves to lower energy side and finally disappears under the $\pi\Sigma$ threshold. Therefore, taking common $a \sim -2$ is essential to reproduce the resonance properties of $\Lambda(1405)$ and the total cross sections of the $K^- p$ scatterings in the low energy region.

	γ	R_c	R_n
experiment	2.36 ± 0.04	0.664 ± 0.011	0.189 ± 0.015
channel dep. a_i	1.73	0.629	0.195
common a	1.80	0.624	0.225
SU(3) breaking	2.19	0.623	0.179

Table II. Threshold branching ratios calculated with the channel dependent a_i , the common $a = -1.96$, and $a = -1.59$ with the SU(3) breaking interaction. The experimental values are taken from Refs. 23), 24).

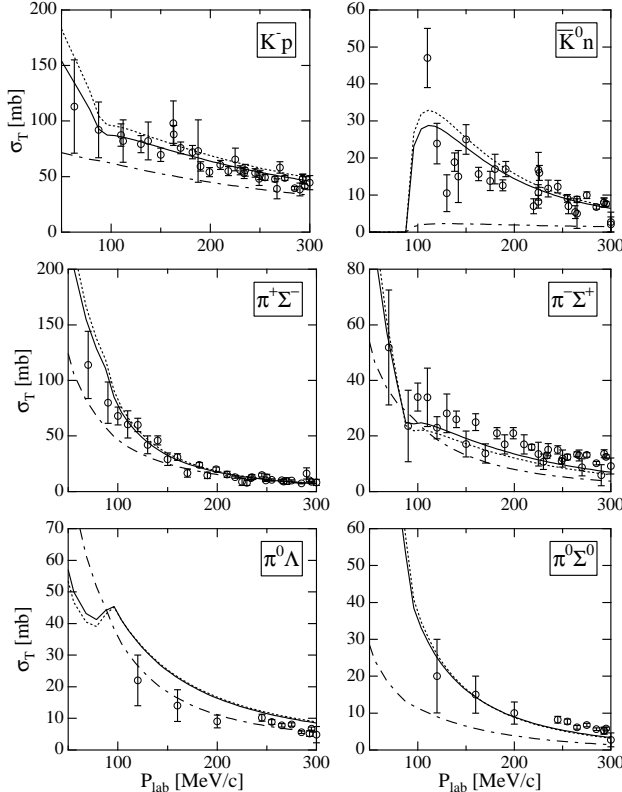


Fig. 4. Total cross sections of $K^- p$ scatterings ($S = -1$) as functions of P_{lab} , the three-momentum of initial K^- in the laboratory frame. Dotted lines show the results with the channel dependent a_i , solid lines show the results with the common $a = -1.96$, and dash-dotted lines show the results with the common $a = -2.6$. Open circles with error bars are experimental data taken from Refs. 25), 26), 27), 28), 29), 30), 31), 32), 33), 34), 35), 36).

3.2. The $S = 0$ channel (πN scattering)

In Ref. 10), the total cross sections of the $\pi^- p$ inelastic scatterings and the resonance properties of the $N(1535)$ were reproduced well by using the channel dependent a_i . After the simplification for f and inelastic channels, the agreement with the data is still acceptable, as shown in Figs. 7 and 8 by dotted lines, as long as the channel dependent a_i are employed. In the T-matrix elements of the πN

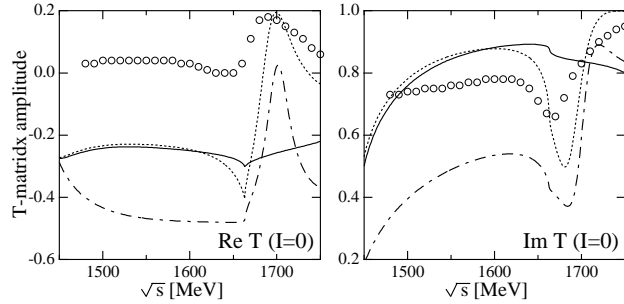


Fig. 5. Real and imaginary parts of the T-matrix amplitude of $\bar{K}N \rightarrow \bar{K}N$ with $I = 0$. Dotted lines show the results with the channel dependent a_i , solid lines show the results with the common $a = -1.96$, and dash-dotted lines show the results with the common $a = -2.6$. Open circles are experimental data taken from Ref. 37).

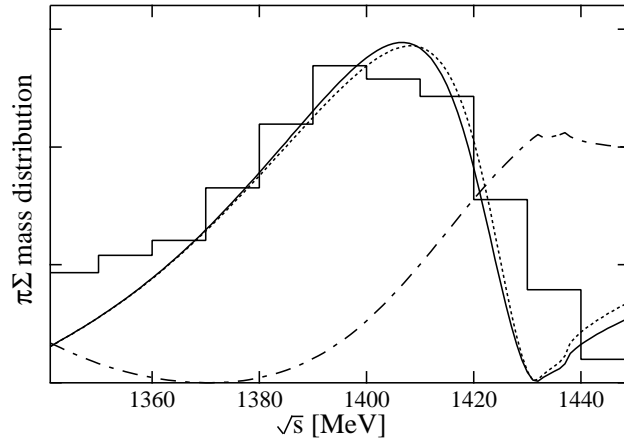


Fig. 6. The mass distributions of the $\pi\Sigma$ channel with $I = 0$. Dotted line shows the result with the channel dependent a_i , solid line shows the result with the common $a = -1.96$, and dash-dotted line shows the result with the common $a = -2.6$. Histogram is experimental data taken from Ref. 38).

scattering in the S_{11} channel, we see a kink structure around the energy $\sqrt{s} \sim 1500$ MeV, which corresponds to the $N(1535)$ resonance.¹⁰⁾

In the previous subsection, we obtained the common subtraction constant $a = -1.96$ with which the $\bar{K}N$ total cross sections and the $\Lambda(1405)$ properties are reproduced well. First, we use this common a for the $S = 0$ channel. It is worth noting that in Ref. 13), $N(1535)$ and $\Lambda(1405)$ were reproduced with the channel independent renormalization scheme. Shown in Figs. 7 and 8 by dash-dotted lines are the results with $a = -1.96$ for the total cross sections of the $\pi^- p \rightarrow \pi^0 \eta$, $K^0 \Lambda$ and $K^0 \Sigma$ scatterings, and the S_{11} T-matrix amplitude of $\pi N \rightarrow \pi N$. As can be seen in Figs. 7 and 8, the results with $a = -1.96$ in the $S = 0$ channel are far from the experimental data. In particular, in the $\pi^- p \rightarrow \eta n$ cross section, the threshold behavior disagrees with the experiment, and the resonance structure of $N(1535)$ disappears. In addi-

tion, as shown in Fig. 8, the T-matrix amplitude of the S_{11} channel is overestimated and an unexpected resonance has been generated at around $\sqrt{s} \sim 1250$ MeV.

Next we search the single optimal subtraction constant within the $S = 0$ channel, since the unnecessary resonance are obtained with $a = -1.96$ at low energy. In order to avoid the appearance of such an unphysical resonance, we determine the common subtraction constant a so as to reproduce observed data up to $\sqrt{s} = 1400$ MeV. The optimal value is found to be $a = 0.53$. The calculated S_{11} amplitude as well as the total cross sections are plotted in Figs. 7 and 8 by the solid lines. With this subtraction constant, the low energy behavior of the S_{11} amplitude of πN scatterings ($\sqrt{s} < 1400$ MeV) is well reproduced. Therefore, the scattering length is also reproduced. However, the $N(1535)$ resonance structure is not still generated. We have also checked that there is no pole in the scattering amplitudes in the second Riemann sheet. Therefore, we conclude that in the $S = 0$ channel we cannot reproduce simultaneously the $N(1535)$ resonance and the S_{11} amplitude at low energy if a single subtraction constant is used within the present approach.

§4. Flavor SU(3) breaking interactions

In the previous studies, it has been found that the channel dependent subtraction constants a_i are crucial in order to reproduce important features of experimental data. In this section, we consider SU(3) breaking terms of the chiral Lagrangian in order to see if the channel dependence in the subtraction constants can be absorbed into those terms. In this way, we are hoping that the number of free parameters could be reduced and that the origin of the channel dependence would be clarified.

4.1. Flavor $SU(3)$ breaking terms in the chiral Lagrangian

Here we introduce the flavor SU(3) breaking effects in the chiral Lagrangian by the quark masses. They are obtained by assuming that the current quark mass matrix \mathbf{m} is transformed under the chiral transformation as $\mathbf{m} \rightarrow R\mathbf{m}L^\dagger$ and $\mathbf{m}^\dagger = \mathbf{m}$. Here we maintain isospin symmetry, namely $\mathbf{m} = \text{diag}(\hat{m}, \hat{m}, m_s)$. Then the SU(3) breaking terms are given uniquely up to order $\mathcal{O}(m_q)$ as²²⁾

$$\begin{aligned} \mathcal{L}_{SB} = & -\frac{Z_0}{2} \text{Tr} \left(d_m \bar{B} \{ \xi \mathbf{m} \xi + \xi^\dagger \mathbf{m} \xi^\dagger, B \} + f_m \bar{B} [\xi \mathbf{m} \xi + \xi^\dagger \mathbf{m} \xi^\dagger, B] \right) \\ & - \frac{Z_1}{2} \text{Tr} (\bar{B} B) \text{Tr} (\mathbf{m} U + U^\dagger \mathbf{m}) , \end{aligned} \quad (4.1)$$

where $f_m + d_m = 1$ and $U(\Phi) = \xi^2 = \exp\{i\sqrt{2}\Phi/f\}$. In this Lagrangian, there are three free parameters, $Z_0, Z_1, f_m/d_m$, which are determined by the baryon masses and the pion-nucleon sigma term, as we see below. For the quark mass, we take $m_s/\hat{m} = 26$, which is determined in ChPT from the meson masses. According to the chiral counting rule, these quark mass terms are regarded as quantities of order $\mathcal{O}(p^2)$, if we assume the Gell-Mann-Oakes-Renner relation,⁶⁰⁾ which tells $m_q \propto m_\pi^2$. In this work, we take into account only the terms of Eq. (4.1), and do not consider other terms of order $\mathcal{O}(p^2)$. We shall explain the reason in the next subsection.

Expanding the Lagrangian (4.1) in powers of the meson fields, the zeroth order

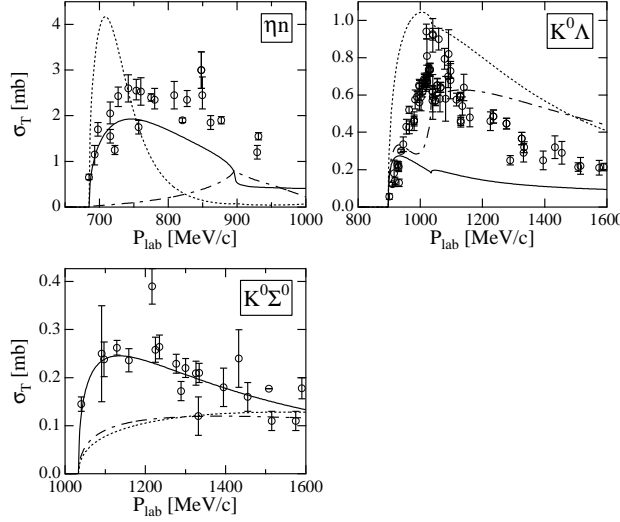


Fig. 7. Total cross sections of $\pi^- p$ scatterings ($S = 0$) as functions of P_{lab} , the three-momentum of initial π^- in the laboratory frame. Dotted lines show the results with channel dependent a_i , dash-dotted lines show the results with the common $a = -1.96$, obtained in $S = -1$, and solid lines show the results with the common $a = 0.53$. Open circles with error bars are experimental data taken from Refs. 39), 40), 41), 42), 43), 44), 45), 46), 47), 48), 49), 50), 51), 52), 53), 54), 55), 56), 57), 58).

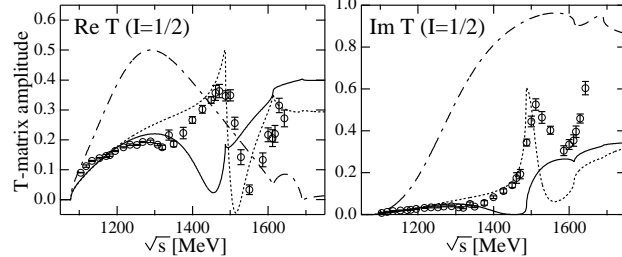


Fig. 8. Real and imaginary parts of the S_{11} T-matrix amplitudes of $\pi N \rightarrow \pi N$. Dotted lines show the results with channel dependent a_i , dash-dotted lines show the results with the common $a = -1.96$, obtained in $S = -1$, and solid lines show the results with the common $a = 0.53$. Open circles with error bars are experimental data taken from Ref. 59).

terms contribute to the baryon mass splitting, which automatically satisfy the Gell-Mann-Okubo (GMO) mass formula.^{61), 62)} By using the mass differences among the octet baryons, we determine the parameters Z_0 and f_m/d_m . The πN sigma term, which we take here $\sigma_{\pi N} = 36.4$ MeV, is used to determine the parameter Z_1 . The resulting parameters are given as

$$Z_0 = 0.528, \quad Z_1 = 1.56, \quad f_m/d_m = -0.31, \quad (4.2)$$

and $M_0 = 759$ MeV in the Lagrangian (2.1).

The meson-baryon interaction Lagrangian with the SU(3) breaking is obtained

by picking up the terms with two meson fields. We find

$$\begin{aligned} \mathcal{L}_{SB}^{(2)} = & \frac{Z_0}{4f^2} \text{Tr} \left(d_m \bar{B} \{ (2\Phi \mathbf{m}\Phi + \Phi^2 \mathbf{m} + \mathbf{m}\Phi^2), B \} + f_m \bar{B} [(2\Phi \mathbf{m}\Phi + \Phi^2 \mathbf{m} + \mathbf{m}\Phi^2), B] \right) \\ & + \frac{Z_1}{f^2} \text{Tr}(\bar{B}B) \text{Tr}(\mathbf{m}\Phi^2). \end{aligned} \quad (4.3)$$

From this Lagrangian the basic interaction is given by

$$\begin{aligned} V_{ij}^{(SB)} = & -\frac{1}{f^2} \left[Z_0 \left((A_{ij}^d d_m + A_{ij}^f f_m) \hat{m} + (B_{ij}^d d_m + B_{ij}^f f_m) m_s \right) \right. \\ & \left. + Z_1 \delta_{ij} D_i^{Z_1} \right] \sqrt{\frac{E_i + M_i}{2M_i}} \sqrt{\frac{E_j + M_j}{2M_j}}. \end{aligned} \quad (4.4)$$

The explicit forms of the coefficients A_{ij} , B_{ij} and D_i are given in Appendix. These interaction terms are independent of the meson momenta unlike the WT interaction (2.9).

Adding Eq. (4.4) to Eq. (2.9) and substituting them into Eq. (2.18), we obtain the unitarized T-matrix with the flavor SU(3) breaking effects as

$$T = \left[1 - \left(V^{(WT)} + V^{(SB)} \right) G \right]^{-1} \left(V^{(WT)} + V^{(SB)} \right). \quad (4.5)$$

Since we have already fitted the all parameters in the chiral Lagrangian, our parameters in the chiral unitary model with the SU(3) breaking effects are only the subtraction constants.

In the chiral Lagrangian, there are other $\mathcal{O}(p^2)$ terms symmetric in the SU(3) flavor in addition to the above breaking terms, if we follow strictly the ordinary chiral counting rule in powers of the pseudoscalar meson momentum p and the quark mass m , where the GMOR relation fixes the ratio of m and p^2 . Indeed, it is known in the chiral perturbation theory at $\mathcal{O}(p^2)$ that the πN scattering length is correctly obtained through a large cancellation between the SU(3) breaking term and symmetric term,^{63),64)} since the lowest order, *i.e.* the Weinberg-Tomozawa term already provides a sufficiently good result. This would imply that the inclusion of only the breaking term would be inconsistent with the cancellation.

However, in the present work, the symmetric terms are not taken into account, because of the following reasons: 1) these terms are not responsible for the symmetry breaking which we would like to study in this paper. 2) the purpose of the present work is to investigate baryon resonances as dynamically generated objects. The symmetric terms of order $\mathcal{O}(p^2)$ would contain the information of resonances⁶⁵⁾ as shown for the role of the ρ meson in the $\pi\pi$ scattering.⁶⁶⁾ The inclusion of some of the symmetric terms would bring intrinsic properties of genuine resonances which are quark originated. 3) in our calculation, the πN scattering length is qualitatively reproduced well without the $\mathcal{O}(p^2)$ symmetric terms, since the subtraction constants in the chiral unitary approach are adjustable parameters determined by the threshold branching ratio Eq. (3.3). Strictly speaking, as argued in Ref. 12), the subtraction constants appear as $\mathcal{O}(p^3)$ quantities in the chiral expansion of the

amplitude obtained by unitary approach, since they are originated from the loop integral. Therefore, they should not cancel the quark mass terms, which are counted as $\mathcal{O}(p^2)$. Nevertheless we have a room to interpret the subtraction constants as containing part of $\mathcal{O}(p^2)$ terms which we do not take into account explicitly, since the parameter fitting is performed for the full amplitudes obtained in the unitarity resummation at the physical threshold and, as we shall see later the threshold ratios are qualitatively reproduced much better than ChPT at the lowest order. This implies that some partial contributions of the symmetric terms are taken into account as constant values at the threshold.

In order to see the third point above, let us introduce another set of parameters a'_i as originated in the \mathcal{T}_{ij}^{-1} term in Eq. (2.11),

$$T_{ij}^{-1}(\sqrt{s}) = \delta_{ij} \left(\tilde{a}_i(s_0) + \frac{s - s_0}{2\pi} \int_{s_i^+}^{\infty} ds' \frac{\rho_i(s')}{(s' - s)(s' - s_0)} \right) + a'_i \delta_{ij} + \mathcal{T}_{ij}^{-1}. \quad (4.6)$$

Here we assume that a'_i form a diagonal matrix in the channel space. Note that the parameters a'_i are introduced as quantities which have nothing to do with the regularization of the loop integral, but they should be determined by ChPT. Now the parameters a'_i can be related to the coefficients of the $\mathcal{O}(p^2)$ symmetric Lagrangian. They are expressed by combinations of the two meson momenta

$$p_1^2, \quad p_2^2, \quad p_1 \cdot p_2, \quad \sigma_{\mu\nu} p_1^\mu p_2^\nu \quad (4.7)$$

with subscripts 1, 2 for the initial and final states, respectively. The last term does not contribute to an s -wave amplitude, and due to the symmetric property under interchanges of 1 and 2 mesons, the coefficients of p_1^2 and p_2^2 should be same. Therefore we have two independent coefficients. It is appropriate to consider the complete set of p^2 terms in the interaction kernel in order to keep strictly the consistency with ChPT and to achieve better agreement with the amplitudes. Once again, however, here we would like to discuss the SU(3) breaking effect on the excited baryons as dynamically generated objects. In our procedure, the SU(3) breaking is considered in the chiral perturbation theory completely, but without properties of genuine resonances.

As seen in Eq. (4.6), the parameters a'_i can be absorbed into the subtraction constants \tilde{a}_i , as $\tilde{a}_i \rightarrow \tilde{a}_i + a'_i$. Furthermore, SU(3) symmetry reduces \tilde{a}_i to a single parameter \tilde{a} . Hence, by adjusting the \tilde{a} parameter, we can use one degree of freedom of a' to fit the low energy data. The introduction of a' is equivalent to the replacement of

$$G \rightarrow G + a'. \quad (4.8)$$

Now we expand the unitarized amplitude (4.5) in terms of small meson momenta p , assuming that a' is an $\mathcal{O}(p^0)$ quantity,

$$\begin{aligned} T &= V^{(WT)} + V^{(SB)} + (V^{(WT)} + V^{(SB)})(G + a')(V^{(WT)} + V^{(SB)}) + \dots \\ &= \underbrace{V^{(WT)}}_{p^1} + \underbrace{V^{(SB)} + V^{(WT)}a'V^{(WT)}}_{p^2} + V^{(WT)}GV^{(WT)} + \dots. \end{aligned} \quad (4.9)$$

The third term in the second line $V^{(WT)}a'V^{(WT)}$ can play a role of interaction derived from the p^2 Lagrangian, and may cancel the $V^{(SB)}$ contribution to the scattering length when we choose $\tilde{a} + a'$ such that the low energy amplitude is reproduced.

4.2. The $S = -1$ channel

We follow the same procedures as in the calculations without the SU(3) breaking terms. First of all, we determine a common subtraction constant a from the threshold branching ratios (3.3). Then the optimal value is found to be $a = -1.59$. With this value, the total cross sections of the K^-p scatterings, the $\pi\Sigma$ mass distribution and the scattering amplitude of $\bar{K}N \rightarrow \bar{K}N$ with $I = 0$ are plotted in Figs. 9,10 and 11 by dash-dotted lines. As seen in the Fig. 9, for all the total cross sections, the inclusion of the SU(3) breaking terms with the common a makes the agreement with data worse, although the threshold branching ratios are produced much better than the previous works, as seen in Table II.

In the $\pi\Sigma$ mass distribution shown in Fig.11 (dash-dotted line), a sharp peak is seen, in obvious contradiction with the observed spectrum, which means that the important resonance structure of $\Lambda(1405)$ has been lost. However, we find two poles of the T-matrix amplitude at $z_1 = 1424 - 1.6i$ and $z_2 = 1389 - 135i$ in the second Riemann sheet. It is reported that there are two poles in the T-matrix amplitude around the energy region of $\Lambda(1405)$ in Refs. 67), 12), 68), 69), 70), 13). A detailed study of the two poles for $\Lambda(1405)$ has been recently done in the viewpoint of the SU(3) flavor symmetry in Ref. 14), and also argued in the reaction processes.^{71), 72)} The inclusion of the SU(3) breaking terms does not change this conclusion, although the positions of the poles change.

We also calculate the total cross sections and the $\pi\Sigma$ mass distribution with the physical values of the meson decay constants, $f_\pi = 93$ MeV, $f_K = 1.22f_\pi$, $f_\eta = 1.3f_\pi$. The calculated results are shown in Figs. 9, 10 and 11 by solid lines. The optimal value of the subtraction constants is $a = -1.68$ to reproduce the threshold branching ratios as $\gamma = 2.35$, $R_c = 0.626$ and $R_n = 0.172$. The SU(3) breaking effect on the meson decay constants is not so large in the total cross sections, as seen in the figures. However, the shape of the peak seen in the $\pi\Sigma$ mass distribution becomes wider than that in the calculation with the averaged meson decay constant.

Indeed we find again two poles in the scattering amplitudes at $z'_1 = 1424 - 2.6i$ and $z'_2 = 1363 - 87i$ in the second Riemann sheet. Compared with the poles z_1 and z_2 obtained in the above calculation, the position of the pole z'_2 moves to lower energy side and approaches the real axis. The reason why the position of z'_2 changes is understood as follows. Since z_2 has large imaginary part, which means large width, and only the $\pi\Sigma$ channel opens in this energy region, the resonance represented by the pole z_2 has strong coupling to the $\pi\Sigma$ channel. This fact implies that the position of the pole z_2 is sensitive to the $\pi\Sigma$ interaction. In the present calculation, the pion decay constant (93 MeV) is smaller than the averaged value (106.95 MeV) used in the above calculation, so that the attractive interaction of $\pi\Sigma$ becomes stronger. It shifts the position of the pole z_2 to lower energy side. Simultaneously, this suppresses the phase space of the decay of the resonance to the $\pi\Sigma$ channel, and hence, the position of the pole approaches the real axis.

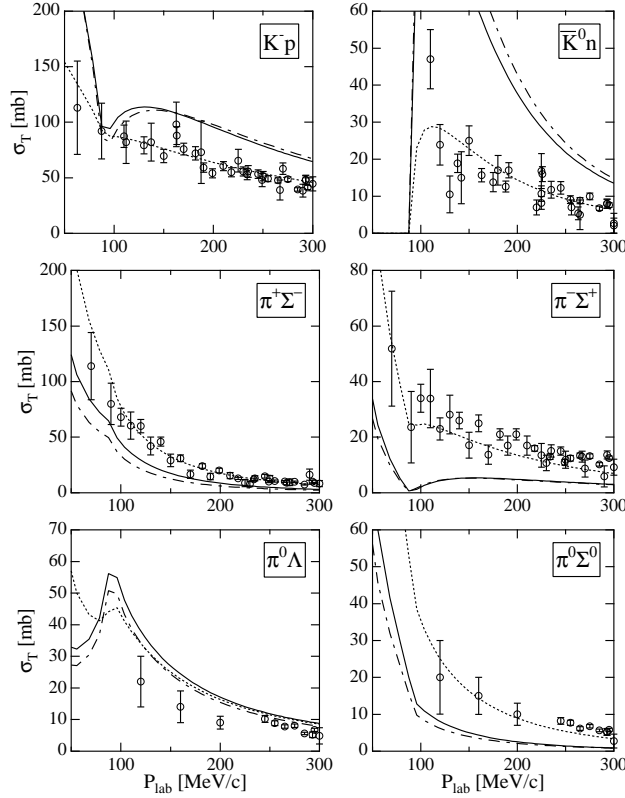


Fig. 9. Total cross sections of $K^- p$ scatterings ($S = -1$) as functions of P_{lab} , the three-momentum of initial K^- in the laboratory frame. Dotted lines show the results with the common $a = -1.96$, dash-dotted lines show the results including the SU(3) breaking with the common $a = -1.59$, and solid lines show the results including the SU(3) breaking and the physical f with the common $a = -1.68$. Open circles with error bars are experimental data taken from Refs. 25), 26), 27), 28), 29), 30), 32), 33), 31), 34), 35), 36).

4.3. The $S = 0$ channel

Here we show calculations in the $S = 0$ channel with the SU(3) breaking terms. With a common $a \sim -1.5$, in which the threshold properties are reproduced well in the $S = -1$ channel, we obtain still the large contribution in the $S_{11} \pi N$ scattering amplitude at the low energy as in the calculation without the SU(3) breaking effects. From this analysis, it is found that the low energy behavior of the πN scatterings cannot be reproduced as long as we use the common $a \sim -2$, even if we introduce the SU(3) breaking effects.

In order to search the optimal value of the common subtraction constant within the $S = 0$ channel, we perform fitting of the T-matrix elements in the πN S_{11} channel in low energy region up to 1400 MeV. We find $a = 1.33$. The results including the SU(3) breaking effects with $a = 1.33$ are shown as dash-dotted lines in Figs. 12 and 13. As seen in Fig. 13, the fitting is well performed up to $\sqrt{s} \sim 1400$ MeV, while,

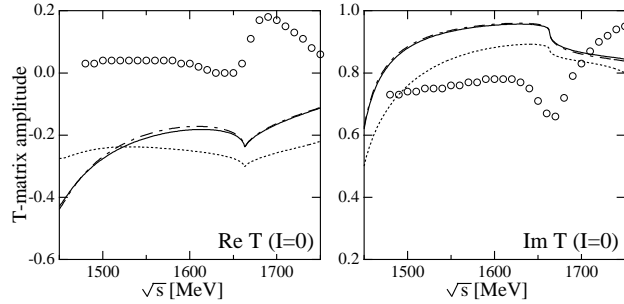


Fig. 10. Real and imaginary parts of the T-matrix amplitude of $\bar{K}N \rightarrow \bar{K}N$ with $I = 0$. Dotted lines show the results with the common $a = -1.96$, dash-dotted lines show the results including the SU(3) breaking with the common $a = -1.59$, and solid lines show the results including the SU(3) breaking and the physical f with the common $a = -1.68$. Open circles are experimental data taken from Ref. 37).

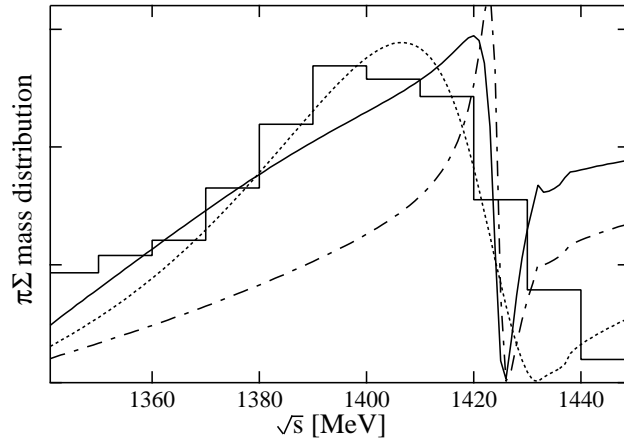


Fig. 11. Mass distributions of the $\pi\Sigma$ channel with $I = 0$. Dotted line shows the result with the common $a = -1.96$, dash-dotted line shows the result including the SU(3) breaking with the common $a = -1.59$, and solid line shows the result including the SU(3) breaking and the physical f with the common $a = -1.68$. Histogram are experimental data taken from Ref. 38).

however, the resonance structure does not appear around the energies of $N(1535)$.

Finally we show the calculations with the physical values of the meson decay constants in Figs. 12 and 13 (solid lines). The optimal value of the common subtraction constant is found to be $a = 2.24$. The results with the physical meson decay constants and $a = 2.24$ are very similar to the calculation with the averaged value of the decay constants and $a = 1.33$. In this sense, the SU(3) breaking effect of the meson decay constant f is absorbed into the change of the common subtraction constant a .

In closing this section, we conclude that even if we introduce the SU(3) breaking effects in the Lagrangian level, the SU(3) breaking in the channel dependent subtraction constants a_i cannot be absorbed into the SU(3) breaking effects in the fundamental interactions in the both $S = -1$ and $S = 0$ channels.

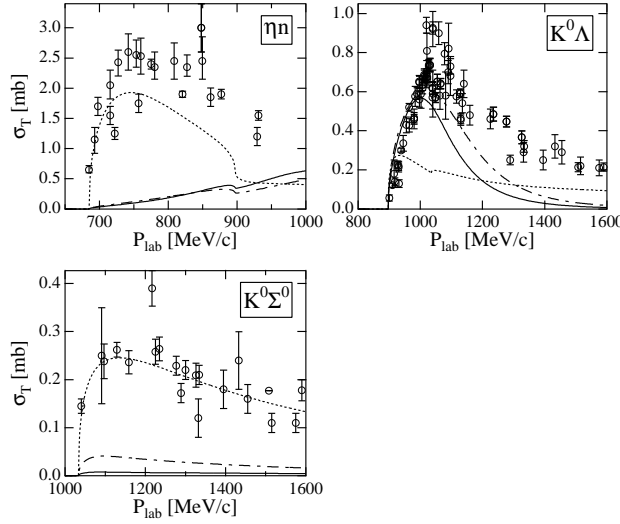


Fig. 12. Total cross sections of $\pi^- p$ scatterings ($S = 0$) as functions of P_{lab} , the three-momentum of initial π^- in the laboratory frame. Dotted lines show the results with the common $a = 0.53$, dash-dotted lines show the results including the SU(3) breaking interaction with the common $a = 1.33$, and solid lines show the results including the SU(3) breaking and the physical f with the common $a = 2.24$. Open circles with error bars are experimental data taken from Refs. 39), 40), 41), 42), 43), 44), 45), 46), 47), 48), 49), 50), 51), 52), 53), 54), 55), 56), 57), 58).

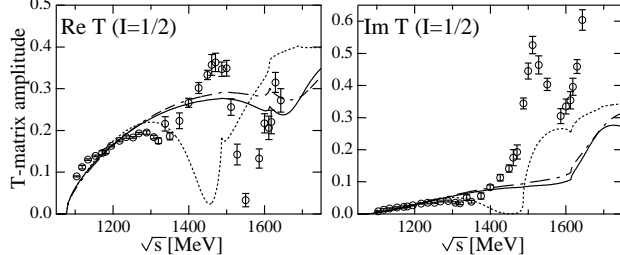


Fig. 13. Real and imaginary parts of the S_{11} T-matrix amplitudes of $\pi N \rightarrow \pi N$. Dotted lines show the results with the common $a = 0.53$, dash-dotted lines show the results including the SU(3) breaking interaction with the common $a = 1.33$, and solid lines show the results including the SU(3) breaking and the physical f with the common $a = 2.24$. Open circles with error bars are experimental data taken from Ref. 59).

§5. Summary and discussions

In this work, first we have tried to use a single common subtraction constant in order to describe meson-baryon scatterings and baryon resonances in a unified way. In the $S = -1$ channel, $a \sim -2$ is fixed from the threshold branching ratios of the $K^- p$ scatterings. With this parameter, the total cross sections of the $K^- p$ scatterings are reproduced well, as well as the mass distribution for $\Lambda(1405)$ is. However, in this case the $\Lambda(1670)$ resonance cannot be reproduced. The subtraction constant $a \sim -2$ corresponds to $\Lambda = 630$ MeV in the three-momentum cut-off

regularization of the meson-baryon loop integral.¹²⁾ This value is consistent with the one often used in single nucleon processes.⁷³⁾ The elementary interaction of the $\bar{K}N$ system is sufficiently attractive, and a resummation of the coupled channel interactions provides the $\Lambda(1405)$ resonance at the correct position, by imposing the unitarity condition and by using the natural value for the cut-off parameter. Hence the wave function of $\Lambda(1405)$ is largely dominated by the $\bar{K}N$ component.

On the other hand, in the $S = 0$ channel, if one uses the natural value for the subtraction constant as in the $S = -1$ channel, the attraction of the meson-baryon interaction becomes so strong that an unexpected resonance is generated at around $\sqrt{s} \sim 1250$ MeV. Therefore, repulsive component is necessary to reproduce the observed πN scattering. The fitted subtraction constant using the low energy πN scattering amplitude is $a \sim 0.5$. With this value, however, the $N(1535)$ resonance is not generated, while the agreement in the cross sections of $\pi^- p \rightarrow \eta n$ is rather good due to the threshold effects.

The unitarized amplitudes are very sensitive to the attractive component of the interaction. The interaction terms of the ChPT alone do not explain all scattering amplitudes simultaneously, but they must be complemented by the subtraction constants in the chiral unitary model. For small a , the interaction becomes more attractive, and for large a , less attractive. For $S = 0$, we need to choose $a \sim 0.5$ in order to suppress the attraction from the πN interaction in contrast to the natural value $a \sim -2$ in the $S = -1$ channel. Therefore, it is not possible to reproduce both the $\Lambda(1405)$ resonance properties and the low energy πN scattering with a common subtraction constant within the present framework.

Generally speaking, the chiral unitary approach is a powerful phenomenological method. It can reproduce cross sections and generate s wave resonances dynamically, once the subtraction constants are determined appropriately, using experimental data. However, it is not straightforward to apply the method to the channels where there are not sufficient experimental data, since they are required to determine the subtraction constants, unless we employ the channel independent renormalization scheme as in Refs. 17), 6), 13).

Next we have introduced the flavor SU(3) breaking Lagrangian, with the hope that the channel dependence in the subtraction constants would be absorbed into the coefficients in the chiral Lagrangian. The coefficients can be determined from other observables, and hence they are more controllable than the subtraction constants which have to be fitted by the experimental data. However, the channel dependence of the subtraction constants in each strangeness channel cannot be replaced by the SU(3) breaking Lagrangian, although we have exhausted possible breaking sources up to order $\mathcal{O}(m_q)$.

Therefore, in the present framework where the Weinberg-Tomozawa term and symmetry breaking terms are taken into account, the suitable choice of the channel dependent subtraction constants is essential. Theoretically, a microscopic explanation of the origin of the channel dependent subtraction constants is very important. One possibility is to consider quark degrees of freedom which can generate genuine resonance states. Another possibility to solve this problem is to employ the interaction terms up to order p^3 with the channel independent renormalization scheme.⁶⁾

Table III. Channels of meson-baryon scatterings. In this work we calculate the channels in $(S = -1, Q = 0)$ and $(S = 0, Q = 0)$.

Y	S	I_3	Q	channels
-2	-3	1	0	$\bar{K}^0\Xi^0$
		0	-1	$K^-\Xi^0, \bar{K}^0\Xi^-$
		-1	-2	$K^-\Xi^-$
-1	-2	$\frac{3}{2}$	1	$\pi^+\Xi^0, \bar{K}^0\Sigma^+$
		$\frac{1}{2}$	0	$\pi^0\Xi^0, \pi^+\Xi^-, \eta\Xi^0, \bar{K}^0\Lambda, \bar{K}^0\Sigma^0, K^-\Sigma^+$
		$-\frac{1}{2}$	-1	$\pi^0\Xi^-, \pi^-\Xi^0, \eta\Xi^-, K^-\Lambda, K^-\Sigma^0, \bar{K}^0\Sigma^-$
		$-\frac{3}{2}$	-2	$\pi^-\Xi^-, K^-\Sigma^-$
0	-1	2	2	$\pi^+\Sigma^+$
		1	1	$\bar{K}^0p, \pi^0\Sigma^+, \pi^+\Sigma^0, \pi^+\Lambda, \eta\Sigma^+, K^+\Xi^0$
		0	0	$K^-p, \bar{K}^0n, \pi^0\Lambda, \pi^0\Sigma^0, \eta\Lambda, \eta\Sigma^0, \pi^+\Sigma^-, \pi^-\Sigma^+, K^+\Xi^-, K^0\Xi^0$
		-1	-1	$K^-n, \pi^0\Sigma^-, \pi^-\Sigma^0, \pi^-\Lambda, \eta\Sigma^-, K^0\Xi^-$
		-2	-2	$\pi^-\Sigma^-$
1	0	$\frac{3}{2}$	2	$\pi^+p, K^+\Sigma^+$
		$\frac{1}{2}$	1	$\pi^0p, \pi^+n, \eta p, K^+\Lambda, K^+\Sigma^0, K^0\Sigma^+$
		$-\frac{1}{2}$	0	$\pi^0n, \pi^-p, \eta n, K^0\Lambda, K^0\Sigma^0, K^+\Sigma^-$
		$-\frac{3}{2}$	-1	$\pi^-n, K^0\Sigma^-$
2	1	1	2	K^+p
		0	1	K^+n, K^0p
		-1	0	K^0n

Further investigations should be explored in order to better understand the nature of baryon resonances.

Acknowledgements

We would like to thank Profs. E. Oset, H. -Ch. Kim and W. Weise for useful discussions.

Appendix A — Coefficients of the $SU(3)$ breaking interaction —

Here we show the coefficients of the flavor $SU(3)$ breaking terms in the meson-baryon interactions. The corresponding Lagrangian is given by

$$\begin{aligned} \mathcal{L}_{SB}^{(2)} = & \frac{Z_0}{4f^2} \text{Tr} \left(d_m \bar{B} \{ (2\Phi \mathbf{m}\Phi + \Phi^2 \mathbf{m} + \mathbf{m}\Phi^2), B \} + f_m \bar{B} [(2\Phi \mathbf{m}\Phi + \Phi^2 \mathbf{m} + \mathbf{m}\Phi^2), B] \right) \\ & + \frac{Z_1}{f^2} \text{Tr}(\bar{B}B) \text{Tr}(\mathbf{m}\Phi^2) . \end{aligned} \quad (\text{A.1})$$

From this Lagrangian, the basic interaction at the tree level is given by

$$\begin{aligned} V_{ij}^{(SB)} = & -\frac{1}{f^2} \left[Z_0 \left((A_{ij}^d d_m + A_{ij}^f f_m) \hat{m} + (B_{ij}^d d_m + B_{ij}^f f_m) m_s \right) \right. \\ & \left. + Z_1 \delta_{ij} D_i^{Z_1} \right] \sqrt{\frac{E_i + M_i}{2M_i}} \sqrt{\frac{E_j + M_j}{2M_j}}, \end{aligned} \quad (\text{A.2})$$

Table IV. Table of $D_i^{Z_1}$.

meson	π	K, \bar{K}	η
$D_i^{Z_1}$	$2\hat{m}$	$\hat{m} + m_s$	$\frac{2}{3}(\hat{m} + 2m_s)$

Table V. Quantum numbers of channels i, j, i' and j'

channel	hypercharge			third component of isospin		
	meson	baryon	total	meson	baryon	total
i	y_i	$Y - y_i$	Y	i_{3i}	$I_3 - i_{3i}$	I_3
j	y_j	$Y - y_j$	Y	i_{3j}	$I_3 - i_{3j}$	I_3
i'	$-y_i$	$-Y + y_i$	$-Y$	$-i_{3i}$	$-I_3 + i_{3i}$	$-I_3$
j'	$-y_j$	$-Y + y_j$	$-Y$	$-i_{3j}$	$-I_3 + i_{3j}$	$-I_3$

where the coefficients A , B and D are the numbers in matrix form and the indices (i, j) denote the channels of the meson-baryon scatterings as shown in Table III.

These channels are specified by two quantum numbers, the hypercharge Y and the third component of isospin I_3 , or equivalently the strangeness S and the electric charge Q , through the Gell-Mann-Nakano-Nishijima relation^{74), 75)}

$$Q = T_3 + \frac{Y}{2}, \quad S = Y - B, \quad (\text{A.3})$$

where the baryon number $B = 1$ for the meson-baryon scatterings.

The coefficient $D_i^{Z_1}$ is specified only by the meson in channel i independently of baryons, because $\text{Tr}(\bar{B}B)$ in the last term of Eq. (A.1) gives a common contribution to all baryons. Also, there is no off-diagonal component when the isospin symmetry is assumed. The explicit form of $D_i^{Z_1}$ is shown in Table IV. The values of the coefficients A and B are shown in the following tables;

- Table VI ($S = 1, Q = 1$)
- Table VII ($S = -3, Q = -1$)
- Tables VIII and IX ($S = 0, Q = 0$)
- Tables X and XI ($S = -2, Q = -1$)
- Tables XII, XIII, XIV and XV ($S = -1, Q = 0$).

From these tables, the coefficients A and B for all the channels can be derived, using symmetry relations.

First, the channels in the same S and different Q are related through the SU(2) Clebsch-Gordan coefficients due to the isospin symmetry. This is the relation among the channels in the block separated by the horizontal lines in table III.

Second, the coefficients of the sector (Y, I_3) are related with those of $(-Y, -I_3)$. Let us consider the channels (i, j) and (i', j') in the sectors (Y, I_3) and $(-Y, -I_3)$, respectively, as shown in Table V. Then the coefficients of the sector $(-Y, -I_3)$ are given by

$$\begin{aligned} A_{i'j'}^d(-Y, -I_3) &= A_{ij}^d(Y, I_3), & A_{i'j'}^f(-Y, -I_3) &= -A_{ij}^f(Y, I_3), \\ B_{i'j'}^d(-Y, -I_3) &= B_{ij}^d(Y, I_3), & B_{i'j'}^f(-Y, -I_3) &= -B_{ij}^f(Y, I_3). \end{aligned} \quad (\text{A.4})$$

Comparing the Table VI ($Y = 2, I_3 = 0$) and Table VII ($Y = -2, I_3 = 0$), we find

Table VI. $A_{ij}^d, A_{ij}^f, B_{ij}^d$ and $B_{ij}^f (S = 1, Q = 1)$

	A_{ij}^d		A_{ij}^f		B_{ij}^d		B_{ij}^f	
	K^+n	K^0p	K^+n	K^0p	K^+n	K^0p	K^+n	K^0p
K^+n	$\frac{1}{2}$	$\frac{1}{2}$	$-\frac{1}{2}$	$\frac{1}{2}$	$\frac{1}{2}$	$\frac{1}{2}$	$-\frac{1}{2}$	$\frac{1}{2}$
K^0p		$\frac{1}{2}$		$-\frac{1}{2}$		$\frac{1}{2}$		$-\frac{1}{2}$

Table VII. $A_{ij}^d, A_{ij}^f, B_{ij}^d$ and $B_{ij}^f (S = -3, Q = -1)$

	A_{ij}^d		A_{ij}^f		B_{ij}^d		B_{ij}^f	
	$K^-\Xi^0$	$\bar{K}^0\Xi^-$	$K^-\Xi^0$	$\bar{K}^0\Xi^-$	$K^-\Xi^0$	$\bar{K}^0\Xi^-$	$K^-\Xi^0$	$\bar{K}^0\Xi^-$
$K^0\Xi^-$	$\frac{1}{2}$	$\frac{1}{2}$	$\frac{1}{2}$	$-\frac{1}{2}$	$\frac{1}{2}$	$\frac{1}{2}$	$\frac{1}{2}$	$-\frac{1}{2}$
$K^-\Xi^0$		$\frac{1}{2}$		$-\frac{1}{2}$		$\frac{1}{2}$		$-\frac{1}{2}$

Table VIII. A_{ij}^d and $A_{ij}^f (S = 0, Q = 0)$

	A_{ij}^d						A_{ij}^f					
	π^0n	π^-p	ηn	$K^0\Lambda$	$K^0\Sigma^0$	$K^+\Sigma^-$	π^0n	π^-p	ηn	$K^0\Lambda$	$K^0\Sigma^0$	$K^+\Sigma^-$
π^0n	1	0	$-\frac{1}{\sqrt{3}}$	$\frac{\sqrt{3}}{8}$	$\frac{3}{8}$	$\frac{3}{4\sqrt{2}}$	1	0	$-\frac{1}{\sqrt{3}}$	$\frac{3\sqrt{3}}{8}$	$-\frac{3}{8}$	$-\frac{3}{4\sqrt{2}}$
π^-p		1	$\sqrt{\frac{2}{3}}$	$-\frac{\sqrt{6}}{8}$	$\frac{3}{4\sqrt{2}}$	0		1	$\sqrt{\frac{2}{3}}$	$-\frac{3\sqrt{6}}{8}$	$-\frac{3}{4\sqrt{2}}$	0
ηn			$\frac{1}{3}$	$-\frac{1}{24}$	$-\frac{1}{8\sqrt{3}}$	$\frac{1}{4\sqrt{6}}$			$\frac{1}{3}$	$-\frac{1}{8}$	$\frac{1}{8\sqrt{3}}$	$-\frac{1}{4\sqrt{6}}$
$K^0\Lambda$				$\frac{5}{6}$	$-\frac{1}{2\sqrt{3}}$	$\frac{1}{\sqrt{6}}$				0	0	0
$K^0\Sigma^0$					$\frac{1}{2}$	0					0	$\frac{1}{\sqrt{2}}$
$K^+\Sigma^-$						$\frac{1}{2}$						$-\frac{1}{2}$

Table IX. B_{ij}^d and $B_{ij}^f (S = 0, Q = 0)$

	B_{ij}^d						B_{ij}^f					
	π^0n	π^-p	ηn	$K^0\Lambda$	$K^0\Sigma^0$	$K^+\Sigma^-$	π^0n	π^-p	ηn	$K^0\Lambda$	$K^0\Sigma^0$	$K^+\Sigma^-$
π^0n	0	0	0	$\frac{1}{8\sqrt{3}}$	$\frac{1}{8}$	$\frac{1}{4\sqrt{2}}$	0	0	0	$\frac{\sqrt{3}}{8}$	$-\frac{1}{8}$	$-\frac{1}{4\sqrt{2}}$
π^-p		0	0	$-\frac{1}{4\sqrt{6}}$	$\frac{1}{4\sqrt{2}}$	0		0	0	$-\frac{\sqrt{6}}{8}$	$-\frac{1}{4\sqrt{2}}$	0
ηn			$\frac{4}{3}$	$\frac{5}{24}$	$\frac{8\sqrt{3}}{24}$	$-\frac{5}{4\sqrt{6}}$				$-\frac{4}{3}$	$\frac{5}{8}$	$-\frac{5}{8\sqrt{3}}$
$K^0\Lambda$				$\frac{5}{6}$	$-\frac{1}{2\sqrt{3}}$	$\frac{1}{\sqrt{6}}$				0	0	0
$K^0\Sigma^0$					$\frac{1}{2}$	0					0	$\frac{1}{\sqrt{2}}$
$K^+\Sigma^-$						$\frac{1}{2}$						$-\frac{1}{2}$

that the relation (A.4) is satisfied. Also, using the relation (A.4), the coefficients of the sector ($S = -2, Q = 0$) are obtained from the tables of the sector ($S = 0, Q = 0$). For example, if we specify (i, j) to be $(\pi^0n, K^0\Lambda)$, the corresponding (i', j') is $(\pi^0\Xi^0, \bar{K}^0\Lambda)$. The coefficients for (i', j') are obtained by $A_{i'j'}^d = \sqrt{3}/8$, $A_{i'j'}^f = -3\sqrt{3}/8$, $B_{i'j'}^d = 1/(8\sqrt{3})$ and $B_{i'j'}^f = -\sqrt{3}/8$. In this way we can derive all the coefficients which are not shown in the tables.

References

- 1) N. Kaiser, P. B. Siegel, and W. Weise, Phys. Lett. **B362**, 23 (1995).
- 2) N. Kaiser, P. B. Siegel, and W. Weise, Nucl. Phys. **A594**, 325 (1995).
- 3) N. Kaiser, T. Waas, and W. Weise, Nucl. Phys. **A612**, 297 (1997).
- 4) B. Krippa, Phys. Rev. **C58**, 1333 (1998).
- 5) E. Oset and A. Ramos, Nucl. Phys. **A635**, 99 (1998).
- 6) M. F. M. Lutz and E. E. Kolomeitsev, Nucl. Phys. **A700**, 193 (2002).

Table X. A_{ij}^d and $A_{ij}^f(S = -2, Q = -1)$

A_{ij}^d							A_{ij}^f						
	$\pi^0 \Xi^-$	$\pi^- \Xi^0$	$\eta \Xi^-$	$K^- \Lambda$	$K^- \Sigma^0$	$\bar{K}^0 \Sigma^-$		$\pi^0 \Xi^-$	$\pi^- \Xi^0$	$\eta \Xi^-$	$K^- \Lambda$	$K^- \Sigma^0$	$\bar{K}^0 \Sigma^-$
$\pi^0 \Xi^-$	1	0	$\frac{1}{\sqrt{3}}$	$-\frac{\sqrt{3}}{8}$	$\frac{3}{8}$	$-\frac{3}{4\sqrt{2}}$	-1	0	$-\frac{1}{\sqrt{3}}$	$\frac{3\sqrt{3}}{8}$	$\frac{3}{8}$	$-\frac{3}{4\sqrt{2}}$	
$\pi^- \Xi^0$		1	$\sqrt{\frac{2}{3}}$	$-\frac{\sqrt{6}}{8}$	$-\frac{3}{4\sqrt{2}}$	0		-1	$-\sqrt{\frac{2}{3}}$	$\frac{3\sqrt{6}}{8}$	$-\frac{3}{4\sqrt{2}}$	0	
$\eta \Xi^-$			$\frac{1}{3}$	$-\frac{1}{24}$	$\frac{1}{8\sqrt{3}}$	$\frac{1}{4\sqrt{6}}$			$-\frac{1}{3}$	$\frac{1}{8}$	$\frac{1}{8\sqrt{3}}$	$\frac{1}{4\sqrt{6}}$	
$K^- \Lambda$				$\frac{5}{6}$	$\frac{1}{2\sqrt{3}}$	$\frac{1}{\sqrt{6}}$				0	0	0	
$K^- \Sigma^0$					$\frac{1}{2}$	0					0	$\frac{1}{\sqrt{2}}$	
$\bar{K}^0 \Sigma^-$						$\frac{1}{2}$						$\frac{1}{2}$	

Table XI. B_{ij}^d and $B_{ij}^f (S = -2, Q = -1)$

	B_{ij}^d						B_{ij}^f					
	$\pi^0 \Xi^-$	$\pi^- \Xi^0$	$\eta \Xi^-$	$K^- \Lambda$	$K^- \Sigma^0$	$K^0 \Sigma^-$	$\pi^0 \Xi^-$	$\pi^- \Xi^0$	$\eta \Xi^-$	$K^- \Lambda$	$K^- \Sigma^0$	$K^0 \Sigma^-$
$\pi^0 \Xi^-$	0	0	0	$-\frac{1}{8\sqrt{3}}$	$\frac{1}{8}$	$-\frac{1}{4\sqrt{2}}$	0	0	0	$\frac{\sqrt{3}}{8}$	$\frac{1}{8}$	$-\frac{1}{4\sqrt{2}}$
$\pi^- \Xi^0$	0	0	$-\frac{1}{4\sqrt{6}}$	$-\frac{1}{4\sqrt{2}}$	0	0	0	0	$\frac{3}{4\sqrt{6}}$	$-\frac{1}{4\sqrt{2}}$	0	0
$\eta \Xi^-$	$\frac{4}{3}$	$\frac{5}{24}$	$-\frac{5}{8\sqrt{3}}$	$-\frac{5}{4\sqrt{6}}$	0	0	$\frac{4}{3}$	$-\frac{5}{8}$	$-\frac{5}{8\sqrt{3}}$	$-\frac{5}{4\sqrt{6}}$	0	0
$K^- \Lambda$		$\frac{5}{6}$	$\frac{1}{2\sqrt{3}}$	$\frac{1}{\sqrt{6}}$	0	0			0	0	0	0
$K^- \Sigma^0$			$\frac{1}{2}$	0	0	0			0	$\frac{1}{\sqrt{2}}$	0	$\frac{1}{2}$
$\bar{K}^0 \Sigma^-$				$\frac{1}{2}$	0	0			0	0	0	$\frac{1}{2}$

Table XII. $A_{ij}^d(S = -1, Q = 0)$

Table XIII. $A_{ij}^f(S = -1, Q = 0)$

Table XIV. $B_{ij}^d(S = -1, Q = 0)$

	$K^- p$	$\bar{K}^0 n$	$\pi^0 \Lambda$	$\pi^0 \Sigma^0$	$\eta \Lambda$	$\eta \Sigma^0$	$\pi^+ \Sigma^-$	$\pi^- \Sigma^+$	$K^+ \Xi^-$	$K^0 \Xi^0$
$K^- p$	1	$\frac{1}{2}$	$-\frac{1}{8\sqrt{3}}$	$\frac{1}{8}$	$\frac{5}{24}$	$-\frac{5}{8\sqrt{3}}$	0	$\frac{1}{4}$	0	0
$\bar{K}^0 n$		1	$\frac{1}{8\sqrt{3}}$	$\frac{1}{8}$	$\frac{5}{24}$	$\frac{5}{8\sqrt{3}}$	$\frac{1}{4}$	0	0	0
$\pi^0 \Lambda$		0	0	0	0	0	0	0	$-\frac{1}{8\sqrt{3}}$	$\frac{1}{8\sqrt{3}}$
$\pi^0 \Sigma^0$			0	0	0	0	0	0	$\frac{1}{8}$	$\frac{1}{8}$
$\eta \Lambda$					$\frac{16}{9}$	0	0	0	$\frac{5}{24}$	$\frac{5}{24}$
$\eta \Sigma^0$						0	0	0	$-\frac{5}{8\sqrt{3}}$	$\frac{5}{8\sqrt{3}}$
$\pi^+ \Sigma^-$							0	0	$\frac{1}{4}$	0
$\pi^- \Sigma^+$								0	0	$\frac{1}{4}$
$K^+ \Xi^-$									1	$\frac{1}{2}$
$K^0 \Xi^0$										1

Table XV. $B_{ij}^f(S = -1, Q = 0)$

	$K^- p$	$\bar{K}^0 n$	$\pi^0 \Lambda$	$\pi^0 \Sigma^0$	$\eta \Lambda$	$\eta \Sigma^0$	$\pi^+ \Sigma^-$	$\pi^- \Sigma^+$	$K^+ \Xi^-$	$K^0 \Xi^0$
$K^- p$	0	$\frac{1}{2}$	$-\frac{\sqrt{3}}{8}$	$-\frac{1}{8}$	$\frac{5}{8}$	$\frac{5}{8\sqrt{3}}$	0	$-\frac{1}{4}$	0	0
$\bar{K}^0 n$		0	$\frac{\sqrt{3}}{8}$	$-\frac{1}{8}$	$\frac{5}{8}$	$-\frac{5}{8\sqrt{3}}$	$-\frac{1}{4}$	0	0	0
$\pi^0 \Lambda$		0	0	0	0	0	0	0	$\frac{\sqrt{3}}{8}$	$-\frac{\sqrt{3}}{8}$
$\pi^0 \Sigma^0$			0	0	0	0	0	0	$\frac{1}{8}$	$\frac{1}{8}$
$\eta \Lambda$					0	0	0	0	$-\frac{5}{8}$	$-\frac{5}{8}$
$\eta \Sigma^0$						0	0	0	$-\frac{5}{8\sqrt{3}}$	$\frac{5}{8\sqrt{3}}$
$\pi^+ \Sigma^-$							0	0	$\frac{1}{4}$	0
$\pi^- \Sigma^+$								0	0	$\frac{1}{4}$
$K^+ \Xi^-$									0	$-\frac{1}{2}$
$K^0 \Xi^0$										0

- 7) S. Weinberg, Physica **A96**, 327 (1979).
- 8) J. Gasser and H. Leutwyler, Nucl. Phys. **B250**, 465 (1985).
- 9) E. Oset, A. Ramos, and C. Bennhold, Phys. Lett. **B527**, 99 (2002).
- 10) T. Inoue, E. Oset, and M. J. Vicente Vacas, Phys. Rev. **C65**, 035204 (2002).
- 11) A. Ramos, E. Oset, and C. Bennhold, Phys. Rev. Lett. **89**, 252001 (2002).
- 12) J. A. Oller and U. G. Meissner, Phys. Lett. **B500**, 263 (2001).
- 13) C. Garcia-Recio, M. F. M. Lutz, and J. Nieves, Phys. Lett. **B582**, 49 (2004).
- 14) D. Jido, J. A. Oller, E. Oset, A. Ramos, and U. G. Meissner, Nucl. Phys. **A725**, 181 (2003).
- 15) T. Hyodo, S. I. Nam, D. Jido, and A. Hosaka, Phys. Rev. **C68**, 018201 (2003).
- 16) E. E. Kolomeitsev and M. F. M. Lutz, Phys. Lett. **B585**, 243 (2004).
- 17) M. F. M. Lutz and E. E. Kolomeitsev, in Proc. of 28th Int. Workshop on Gross Properties of Nuclei and Nuclear Excitations: Hadrons in Dense Matter, Hirschegg, Austria, 16-22 January 2000, nucl-th/0004021.
- 18) D. Jido, E. Oset, and A. Ramos, Phys. Rev. **C66**, 055203 (2002).
- 19) A. Gomez Nicola, J. Nieves, J. R. Pelaez, and E. Ruiz Arriola, Phys. Lett. **B486**, 77 (2000).
- 20) G. F. Chew and S. Mandelstam, Phys. Rev. **119**, 467 (1960).
- 21) U.-G. Meissner and J. A. Oller, Nucl. Phys. **A673**, 311 (2000).
- 22) For example, J. F. Donoghue, E. Golowich, and B. R. Holstein, *Dynamics of the standard model* (Cambridge University Press, London, 1992).
- 23) R. J. Nowak *et al.*, Nucl. Phys. **B139**, 61 (1978).
- 24) D. N. Tovee *et al.*, Nucl. Phys. **B33**, 493 (1971).
- 25) T. S. Mast *et al.*, Phys. Rev. **D14**, 13 (1976).
- 26) J. Ciborowski *et al.*, J. Phys. **G8**, 13 (1982).
- 27) R. O. Bangerter *et al.*, Phys. Rev. **D23**, 1484 (1981).

28) T. S. Mast *et al.*, Phys. Rev. **D11**, 3078 (1975).

29) M. Sakitt *et al.*, Phys. Rev. **139**, B719 (1965).

30) M. B. Watson, M. Ferro-Luzzi, and R. D. Tripp, Phys. Rev. **131**, 2248 (1963).

31) J. K. Kim, Phys. Rev. Lett. **14**, 29 (1965).

32) M. Ferro-Luzzi, R. D. Tripp, and M. B. Watson, Phys. Rev. Lett. **8**, 28 (1962).

33) M. Csejthely-Barth *et al.*, Phys. Lett. **16**, 89 (1965).

34) J. Paul Nordin, Phys. Rev. **123**, 2168 (1961).

35) W. Kittel, G. Ptter, and I. Wacek, Phys. Lett. **21**, 349 (1966).

36) H. Going, Nuovo Cim. **16**, 848 (1960).

37) Rutherford-London, G. P. Gopal *et al.*, Nucl. Phys. **B119**, 362 (1977).

38) R. J. Hemingway, Nucl. Phys. **B253**, 742 (1985).

39) M. Batinic, I. Slaus, A. Svarc, and B. M. K. Nefkens, Phys. Rev. **C51**, 2310 (1995).

40) J. C. Hart *et al.*, Nucl. Phys. **B166**, 73 (1980).

41) D. H. Saxon *et al.*, Nucl. Phys. **B162**, 522 (1980).

42) R. D. Baker *et al.*, Nucl. Phys. **B145**, 402 (1978).

43) R. D. Baker *et al.*, Nucl. Phys. **B141**, 29 (1978).

44) B. Nelson *et al.*, Phys. Rev. Lett. **31**, 901 (1973).

45) D. W. Thomas, A. Engler, H. E. Fisk, and R. W. Kraemer, Nucl. Phys. **B56**, 15 (1973).

46) J. J. Jones *et al.*, Phys. Rev. Lett. **26**, 860 (1971).

47) T. O. Binford *et al.*, Phys. Rev. **183**, 1134 (1969).

48) O. Van Dyck *et al.*, Phys. Rev. Lett. **23**, 50 (1969).

49) T. M. Knasel *et al.*, Phys. Rev. **D11**, 1 (1975).

50) R. L. Crolius *et al.*, Phys. Rev. **155**, 1455 (1967).

51) J. Keren, Phys. Rev. **133**, B457 (1963).

52) L. L. Yoder, C. T. Coffin, D. I. Meyer, and K. M. Terwilliger, Phys. Rev. **132**, 1778 (1963).

53) L. B. Leipuner and R. K. Adair, Phys. Rev. **109**, 1358 (1958).

54) L. Bertanza *et al.*, Phys. Rev. Lett. **8**, 332 (1962).

55) F. S. Crawford *et al.*, Phys. Rev. Lett. **3**, 394 (1959).

56) R. T. V. de Walle, C. L. A. Pols, D. J. Schotanus, H. J. G. M. Tiecke, and D. Z. Toet, Nuovo Cim. **A53**, 745 (1968).

57) O. Goussu *et al.*, Nuovo Cim. **42A**, 606 (1966).

58) F. Eisler *et al.*, Nuovo Cim. **10**, 468 (1958).

59) Center of Nuclear Study, <http://gwdac.phys.gwu.edu> .

60) M. Gell-Mann, R. J. Oakes, and B. Renner, Phys. Rev. **175**, 2195 (1968).

61) M. Gell-Mann, Phys. Rev. **125**, 1067 (1962).

62) S. Okubo, Prog. Theor. Phys. **27**, 949 (1962).

63) V. Bernard, N. Kaiser, and U. G. Meissner, Phys. Lett. **B309**, 421 (1993).

64) V. Bernard, N. Kaiser, and U. G. Meissner, Phys. Rev. **C52**, 2185 (1995).

65) V. Bernard, N. Kaiser, and U.-G. Meissner, Int. J. Mod. Phys. **E4**, 193 (1995).

66) G. Ecker, J. Gasser, A. Pich, and E. de Rafael, Nucl. Phys. **B321**, 311 (1989).

67) P. J. Fink, G. He, R. H. Landau, and J. W. Schnick, Phys. Rev. **C41**, 2720 (1990).

68) D. Jido, A. Hosaka, J. C. Nacher, E. Oset, and A. Ramos, Phys. Rev. **C66**, 025203 (2002).

69) C. Garcia-Recio, J. Nieves, E. Ruiz Arriola, and M. J. Vicente Vacas, Phys. Rev. **D67**, 076009 (2003).

70) S. I. Nam, H. -Ch. Kim, T. Hyodo, D. Jido, and A. Hosaka, hep-ph/0309017.

71) T. Hyodo, A. Hosaka, E. Oset, A. Ramos, and M. J. Vicente Vacas, Phys. Rev. **C68**, 065203 (2003).

72) T. Hyodo, A. Hosaka, M. J. V. Vacas, and E. Oset, nucl-th/0401051, Phys. Lett. B, in press.

73) C. Bennhold and H. Tanabe, Nucl. Phys. **A530**, 625 (1991).

74) M. Gell-Mann, Phys. Rev. **92**, 833 (1954).

75) T. Nakano and K. Nishijima, Prog. Theor. Phys. **10**, 581 (1954).